Catheter Ablation of Cardiac Arrhythmias

SECOND EDITION

Edited by

Shoei K. Stephen Huang, MD
Professor of Medicine
College of Medicine
Texas A&M University Health Science Center;
Section of Cardiac Electrophysiology and Pacing
Scott & White Heart and Vascular Institute
Scott & White Healthcare
Temple, Texas

Distinguished Chair, Professor of Medicine
College of Medicine
Tzu Chi University
Hualien, Taiwan

Mark A. Wood, MD
Professor of Medicine
Assistant Director
Cardiac Electrophysiology Laboratory
Virginia Commonwealth University Medical Center
Richmond, Virginia

ELSEVIER
SAUNDERS

ENDYMED EXHIBIT 1022 - 1/20
EndyMed v Serendia
IPR2024-00842

ELSEVIER
SAUNDERS

1600 John F. Kennedy Blvd.
Ste 1800
Philadelphia, PA 19103-2899

CATHETER ABLATION OF CARDIAC ARRHYTHMIAS ISBN: 978-1-4377-1368-8

Copyright © 2011, 2006 by Saunders, an imprint of Elsevier Inc. All rights reserved.

No part of this publication may be reproduced or transmitted in any form or by any means, electronic or mechanical, including photocopying, recording, or any information storage and retrieval system, without permission in writing from the publisher. Details on how to seek permission, further information about the Publisher's permissions policies and our arrangements with organizations such as the Copyright Clearance Center and the Copyright Licensing Agency, can be found at our website: www.elsevier.com/permissions.

This book and the individual contributions contained in it are protected under copyright by the Publisher (other than as may be noted herein).

Notices

Knowledge and best practice in this field are constantly changing. As new research and experience broaden our understanding, changes in research methods, professional practices, or medical treatment may become necessary.

Practitioners and researchers must always rely on their own experience and knowledge in evaluating and using any information, methods, compounds, or experiments described herein. In using such information or methods they should be mindful of their own safety and the safety of others, including parties for whom they have a professional responsibility.

With respect to any drug or pharmaceutical products identified, readers are advised to check the most current information provided (i) on procedures featured or (ii) by the manufacturer of each product to be administered, to verify the recommended dose or formula, the method and duration of administration, and contraindications. It is the responsibility of practitioners, relying on their own experience and knowledge of their patients, to make diagnoses, to determine dosages and the best treatment for each individual patient, and to take all appropriate safety precautions.

To the fullest extent of the law, neither the Publisher nor the authors, contributors, or editors assume any liability for any injury and/or damage to persons or property as a matter of products liability, negligence or otherwise, or from any use or operation of any methods, products, instructions, or ideas contained in the material herein.

Library of Congress Cataloging-in-Publication Data
Catheter ablation of cardiac arrhythmias / edited by Shoei K. Stephen Huang, Mark A. Wood. – 2nd ed.
p. ; cm.
Includes bibliographical references and index.
ISBN 978-1-4377-1368-8 (hardcover)
1. Catheter ablation. 2. Arrhythmia–Surgery. I. Huang, Shoei K. II. Wood, Mark A.
[DNLM: 1. Tachycardia–therapy. 2. Arrhythmias, Cardiac–therapy. 3. Catheter Ablation–methods. WG 330]
RD598.35.C39C36 2011
617.4'12–dc22

2010039806

Executive Publisher: Natasha Andjelkovic
Senior Developmental Editor: Mary Beth Murphy
Publishing Services Manager: Anne Altepeter
Team Manager: Radhika Pallamparthy
Senior Project Manager: Doug Turner
Project Manager: Preethi Kerala Varma
Designer: Steve Stave

Working together to grow
libraries in developing countries
www.elsevier.com | www.bookaid.org | www.sabre.org
ELSEVIER BOOK AID International Sabre Foundation

Printed in Canada

Last digit is the print number: 9 8 7 6 5 4 3 2 1

ENDYMED EXHIBIT 1022 - 2/20

1 Biophysics of Radiofrequency Lesion Formation

David E. Haines

Key Points

Radiofrequency (RF) energy induces thermal lesion formation through resistive heating of myocardial tissue. Tissue temperatures of 50°C or higher are necessary for irreversible injury.

Under controlled conditions, RF lesion size is directly proportional to delivered power, electrode-tissue interface temperature, electrode diameter, and contact pressure.

Power density declines with the square of distance from the source and tissue temperature declines inversely with distance from the heat source.

The ultimate RF lesion size is determined by the zone of acute necrosis as well as the region of microvascular injury.

Electrode cooling reduces the efficiency of tissue heating. For a fixed energy delivery, blood flow over the electrode-tissue interface reduces lesion size by convective tissue cooling. Cooled ablation increases lesion size by increasing the power that can be delivered before limiting electrode temperatures are achieved.

When Huang and colleagues first introduced radiofrequency (RF) catheter ablation in 1985[1] as a potentially useful modality for the management of cardiac arrhythmias,[2] few would have predicted its meteoric rise. In the past two decades, it has become one of the most useful and widely employed therapies in the field of cardiac electrophysiology. RF catheter ablation has enjoyed a high efficacy and safety profile, and indications for its use continue to expand. Improvements in catheter design have continued to enhance the operator's ability to target the arrhythmogenic substrate, and modifications in RF energy delivery and electrode design have resulted in more effective energy coupling to the tissue. It is likely that most operators view RF catheter ablation as a "black box" in that once the target is acquired, they need only push the button on the RF generator. However, gaining insight into the biophysics of RF energy delivery and the mechanisms of tissue injury in response to this intervention will help the clinician optimize catheter ablation and ultimately may enhance its efficacy and safety.

Biophysics of Tissue Heating

Resistive Heating

RF energy is a form of alternating electrical current that generates a lesion in the heart by electrical heating of the myocardium. A common form of RF ablation found in the medical environment is the electrocautery employed for tissue cutting and coagulation during surgical procedures. The goal of catheter ablation with RF energy is to effectively transform electromagnetic energy into thermal energy in the tissue and destroy the arrhythmogenic tissues by heating them to a lethal temperature. The mode of tissue heating by RF energy is resistive (electrical) heating. As electrical current passes through a resistive medium, the voltage drops, and heat is produced (similar to the heat that is created in an incandescent light bulb). The RF electrical current is typically delivered in a unipolar fashion with completion of the circuit through an indifferent electrode placed on the skin. Typically, an oscillation frequency of 500 kHz is selected. Lower frequencies are more likely to stimulate cardiac muscle and nerves, resulting in arrhythmia generation and pain sensation. Higher frequencies will result in tissue heating, but in the megahertz range the mode of energy transfer changes from electrical (resistive) heating to dielectric heating (as observed with microwave energy). With very high frequencies, conventional electrode catheters become less effective at transferring the electromagnetic energy to the tissue, and complex and expensive catheter "antenna" designs must be employed.[3]

Resistive heat production within the tissue is proportional to the RF power density and that, in turn, is proportional to the square of the current density (Table 1-1). When RF energy is delivered in a unipolar fashion, the current distributes radially from the source. The current density decreases in proportion to the square of the

This material may be protected by Copyright law (Title 17 U.S. Code)

ENDYMED EXHIBIT 1022 - 3/20

TABLE 1-1

EQUATIONS DESCRIBING BIOPHYSICS OF RADIOFREQUENCY ABLATION

$V = I R$	Ohm's law: V, voltage; I, current; R, resistance
$\text{Power} = V I (\cos \acute{\alpha})$	Cos ά represents the phase shift between voltage (V) and current (I) in alternating current
$\text{Current density} = I/4 \pi r^2$	I, total electrode current; r, distance from electrode center
$H \approx p I^2/16 \pi^2 r^4$	H, heat production per unit volume of tissue; p, tissue resistivity; I, current; r, distance from the electrode center
$T(t) = T_{ss} + (T_{initial} - T_{ss})e^{-t/\tau}$	Monoexponential relationship between tissue temperature (T) and duration of radiofrequency energy delivery (t): $T_{initial}$, starting tissue temperature; T_{ss}, tissue temperature at steady state; τ, time constant
$r/r_i = (t_o - T)/(t - T)$	Relationship between tissue temperature and distance from heat source in ideal system: r, distance from center of heat source; r_i, radius of heat source; t_o, temperature at electrode tissue interface; T, basal tissue temperature; t, temperature at radius r

distance from the RF electrode source. Thus, direct resistive heating of the tissue decreases proportionally with the distance from the electrode to the fourth power (Fig. 1-1). As a result, only the narrow rim of tissue in close contact with the catheter electrode (2 to 3 mm) is heated directly. All heating of deeper tissue layers occurs passively through heat conduction.[4] If higher power levels are used, the depth of direct resistive heating will increase, and the volume and radius of the virtual heat source will increase as well.

Thermal Conduction

Most of the tissue heating resulting in lesion formation during RF catheter ablation occurs as a result of thermal conduction from the direct resistive heat source. Transfer of heat through tissue follows basic thermodynamic principles and is represented by the bioheat transfer equation.[5] The tissue temperature change with increasing distance from the heat source is called the *radial temperature gradient*. At onset of RF energy delivery, the temperature is very high at the source of heating and falls off rapidly over a short distance (Fig 1.1 and **Videos 1-1 and 1-2**). As time progresses, more thermal energy is transferred to deeper tissue layers by means of thermal conduction. The rise of tissue temperature at any given distance from the heat source increases in a monoexponential fashion over time. Sites close to the heat source have a rapid rise in temperature (a short half-time of temperature rise), whereas sites remote from the source heat up more slowly.[6] Eventually, the entire electrode-tissue system reaches steady state, meaning that the amount of energy entering the tissue at the thermal source equals the amount of energy that is being dissipated at the tissue margins beyond the lesion border. At steady state, the radial temperature gradient becomes constant. If RF power delivery is interrupted before steady state is achieved, tissue temperature will continue to rise in deeper tissue planes as a result of thermal conduction from more superficial layers heated to higher temperatures. In one study, the duration of continued temperature rise at the lesion border zone after a 10-second RF energy delivery was 6 seconds. The temperature rose an additional 3.4°C and remained above the temperature recorded at the termination of energy delivery for more than 18 seconds. This phenomenon, termed *thermal latency*, has important clinical implications because active ablation, with beneficial or adverse effects, will continue for a period of time despite cessation of RF current flow.[7]

Because the mechanism of tissue injury in response to RF ablation is thermal, the final peak temperature at the border zone of the ablative lesion should be relatively constant. Experimental studies predict this temperature with hyperthermic ablation to be about 50°C.[3] This is called the *isotherm of irreversible tissue injury*. The point at which the radial temperature gradient crosses the 50°C isothermal line defines the lesion radius in that dimension. One may predict the three-dimensional temperature gradients with thermodynamic modeling and finite element analysis and by doing so can predict the anticipated lesion dimensions and geometry with the 50°C isotherm. In an idealized medium of uniform thermal conduction without convective heat loss, a number of relationships can be defined using boundary conditions when a steady-state radial temperature gradient is achieved. In this theoretical model, it is predicted that radial temperature gradient is inversely proportional to the distance from the heat source. The 50°C isotherm boundary (lesion radius) increases in distance from the source in direct proportion to the temperature at that source. It was predicted, then demonstrated experimentally, that in the absence of significant heat loss due to convective cooling, the lesion depth and diameter are best predicted by the electrode-tissue interface temperature.[4] In the clinical setting, however, the opposing effects of convective cooling by circulating blood flow diminish the value of electrode-tip temperature monitoring to assess lesion size.

The idealized thermodynamic model of catheter ablation by tissue heating predicted, then demonstrated, that the radius of the lesion is directly proportional to the radius of the heat source (Fig. 1-2).[8] When one considers the virtual heat source radius as the shell of direct resistive heating in tissue contiguous to the electrode, it is not surprising that larger electrode diameter, length, and contact area all result in a larger source radius and larger lesion size, and that this may result in enhanced procedural success. Higher power delivery not only increases the source temperature but also increases the radius of the heat source, thereby increasing lesion size in two ways. These theoretical means of increasing efficacy of RF catheter ablation have been realized in the clinical setting with large-tip catheters and cooled-tip catheters.[9–11]

The relationship of ablation catheter distance from the ablation target to the power requirements for clinical effect

ENDYMED EXHIBIT 1022 - 4/20

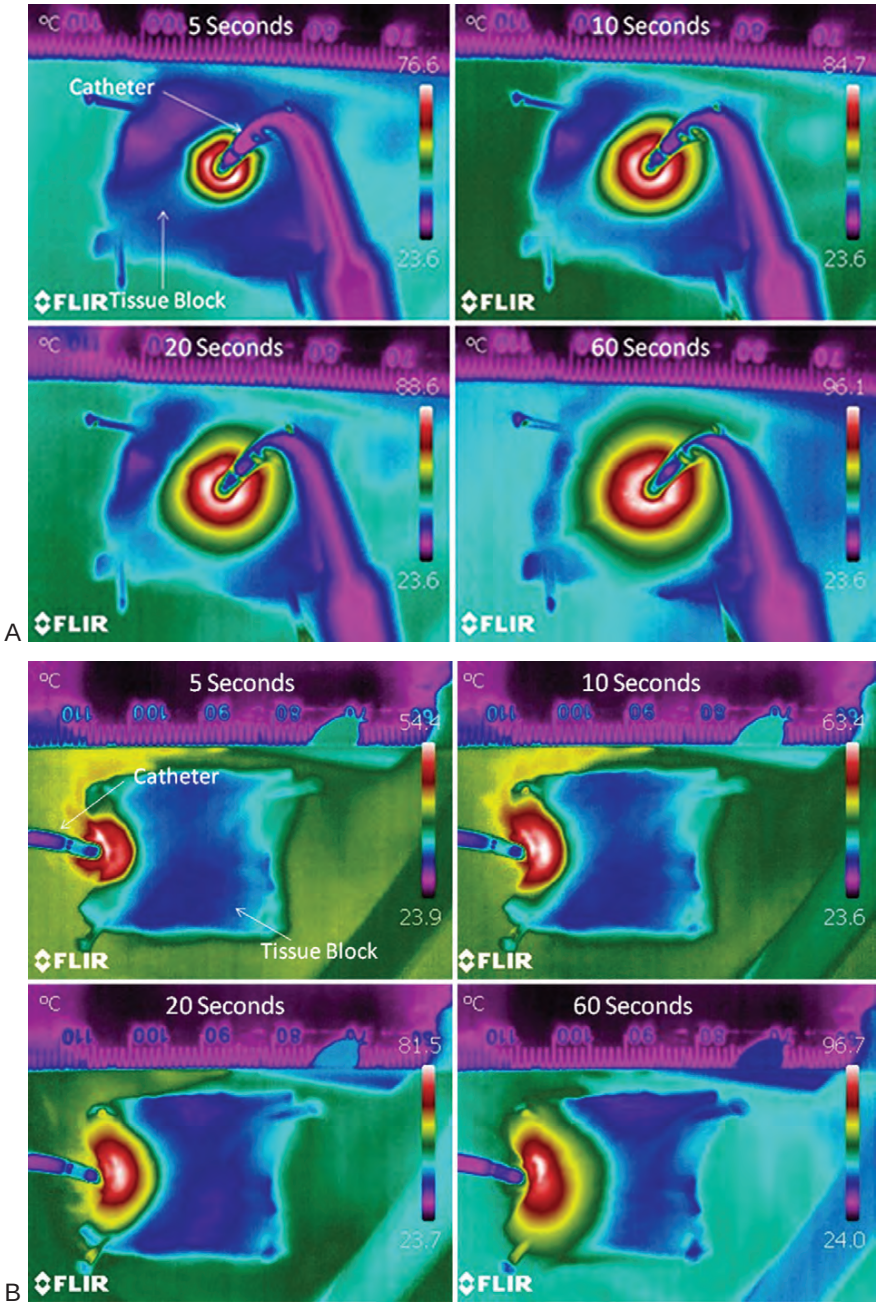

FIGURE 1-1. Infrared thermal imaging of tissue heating during radiofrequency ablation with a closed irrigation catheter. Power is delivered at 30 W to blocks of porcine myocardium in a tissue bath. The surface of the tissue is just above the fluid level to permit thermal imaging of tissue and not the fluid. Temperature scale (*right*) and a millimeter scale (*top*) are shown in each panel. **A,** Viewed from the surface, there is radial heating of the tissue from the electrode. **B,** Tissue heating visualized in cross section. The electrode is partially submerged in the fluid bath and perpendicular to the upper edge of the tissue. In both cases, very high tissue temperatures (>96°C) are achieved at 60 seconds because of the absence of fluid flow over the tissue surface.

were tested in a Langendorff-perfused canine heart preparation. Catheter ablation of the right bundle branch was attempted at varying distances, and while delivered, power was increased in a stepwise fashion. The RF power required to block right bundle branch conduction increased exponentially with increasing distance from the catheter. At a distance of 4 mm, most RF energy deliveries reached the threshold of impedance rise before block was achieved. When pulsatile flow was streamed past the ablation electrode, the power requirements to cause block increased fourfold.[12] Thus, the efficiency of heating diminished with cooling from circulating blood, and small increases in distances from the ablation target corresponded with large increases in ablation power requirements, emphasizing the importance of optimal targeting for successful catheter ablation.

ENDYMED EXHIBIT 1022 - 5/20

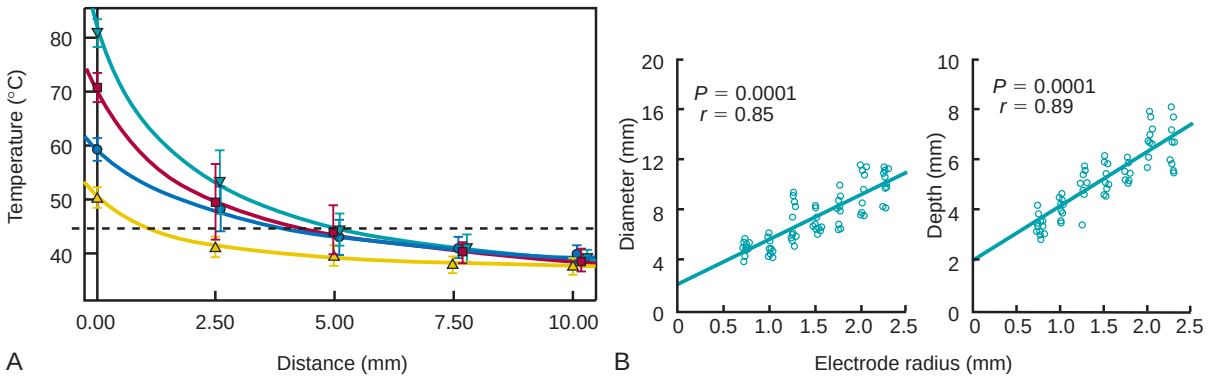

FIGURE 1-2. A, Radial temperature gradients measured during in vitro catheter ablation with source temperatures varying from 50° to 80°C. The tissue temperature falls in an inverse proportion to distance. The *dashed line* represents the 50°C isothermal line. The point at which the radial temperature gradient crosses the 50°C isotherm determines the boundary of the lesion. A higher source temperature results in a greater lesion depth. **B,** Lesion depth and diameter are compared to the electrode radius in temperature feedback power controlled radiofrequency ablation. A larger-diameter ablation electrode results in higher power delivery and a proportional increase in lesion dimension. *(From Haines DE, Watson DD, Verow AF. Electrode radius predicts lesion radius during radiofrequency energy heating: validation of a proposed thermodynamic model.* Circ Res. *1990;67:124–129. With permission.)*

Sudden Impedance Rise

In a uniform medium, the steady-state radial temperature gradient should continue to shift deeper into the medium as the source temperature increases. A very high source temperature, therefore, should theoretically yield a very deep 50°C isotherm temperature and, in turn, very large ablative lesions. Unfortunately, this process is limited in the biologic setting by the formation of coagulum and char at the electrode-tissue interface if temperatures exceed 100°C. At 100°C, blood literally begins to boil. This can be observed in the clinical setting with generation of showers of microbubbles if tissue heating is excessive.[13] As the blood and tissue in contact with the electrode catheter desiccate, the residue of denatured proteins adheres to the electrode surface. These substances are electrically insulating and result in a smaller electrode surface area available for electrical conduction. In turn, the same magnitude of power is concentrated over a smaller surface area, and the power density increases. With higher power density, the heat production increases, and more coagulum forms. Thus, in a positive-feedback fashion, the electrode becomes completely encased in coagulum within 1 to 2 seconds. In a study testing ablation with a 2-mm-tip electrode in vitro and in vivo, a measured temperature of at least 100°C correlated closely with a sudden rise in electrical impedance (Fig. 1-3).[14] Modern RF energy ablation systems all have an automatic energy cutoff if a rapid rise in electrical impedance is observed. Some experimenters have described soft thrombus that accumulates when temperatures exceed 80°C.[15] This is likely due to blood protein denaturation and accumulation, but fortunately appears to be more of a laboratory phenomenon than one observed in the clinical setting. When high temperatures and sudden rises in electrical impedance are observed, there is concern about the accumulation of char and coagulum, with the subsequent risk for char embolism. Anticoagulation and antiplatelet therapies have been proposed as preventative measures,[16] but avoidance of excessive heating at the electrode-tissue interface remains the best strategy to avoid this risk.

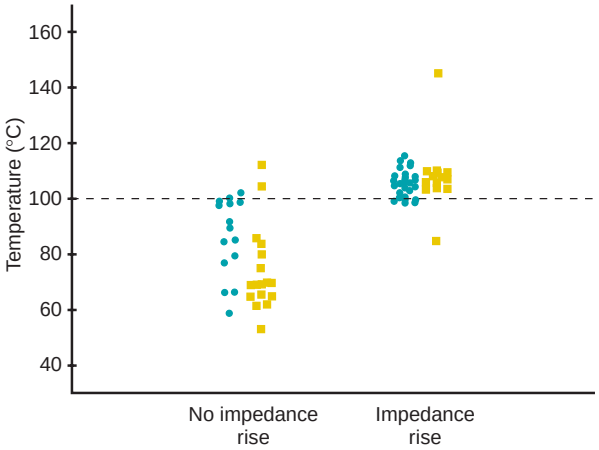

FIGURE 1-3. The association of measured electrode-tip temperature and sudden rise in electrical impedance is shown in this study of radiofrequency catheter ablation with a 2-mm-tip ablation electrode in vitro (*blue circles*) and in vivo (*yellow squares*). The peak temperature recorded at the electrode-tissue interface is shown. Almost all ablations without a sudden rise in electrical impedance had a peak temperature of 100°C or less, whereas all but one ablation manifesting a sudden rise in electrical impedance had peak temperatures of 100°C or more. *(From Haines DE, Verow AF. Observations on electrode-tissue interface temperature and effect on electrical impedance during radiofrequency ablation of ventricular myocardium.* Circulation. *1990;82:1034–1038. With permission.)*

Convective Cooling

The major thermodynamic factor opposing the transfer of thermal energy to deeper tissue layers is convective cooling. Convection is the process whereby heat is distributed through a medium rapidly by active mixing of that medium. With the case of RF catheter ablation, the heat is produced by resistive heating and transferred to deeper layers by thermal conduction. Simultaneously, the heat is conducted back into the circulating blood pool and metal electrode tip. Because the blood is moving rapidly past the electrode and over the endocardial surface, and because water (the main constituent of blood) has a high heat capacity, a large amount of the heat produced at the site of ablation can

ENDYMED EXHIBIT 1022 - 6/20

be carried away by the blood. Convective cooling is such an important factor that it dominates the thermodynamics of catheter ablation.[17] Efficiency of energy coupling to the tissue can be as low as 10%, depending on electrode size, catheter stability, and position relative to intracavitary blood flow.[18] Unstable, sliding catheter contact results in significant tip cooling and decreased efficiency of tissue heating.[19] This is most often observed with ablation along the tricuspid or mitral valve annuli.

Paradoxically, the convective cooling phenomenon has been used to increase lesion size. As noted earlier, maximal power delivery during RF ablation is limited by the occurrence of boiling and coagulum formation at the electrode tip. However, if the tip is cooled, a higher magnitude of power may be delivered without a sudden rise in electrical impedance. The higher magnitude of power increases the depth of direct resistive heating and, in turn, increases the radius of the effective heat source. In addition, higher temperatures are achieved 3 to 4 mm below the surface, and the entire radial temperature curve is shifted to a higher temperature over greater tissue depths. The result is a greater 50°C isotherm radius and a greater depth and diameter of the lesion. Nakagawa demonstrated this phenomenon in a blood-superfused exposed thigh muscle preparation. In this study, intramural tissue temperatures 3.5 mm from the surface averaged 95°C with an irrigated-tip catheter despite a mean electrode-tissue interface temperature of 69°C. Lesion depths were 9.9 mm compared with 6.1 mm in a comparison group of temperature-feedback power control delivery and no electrode irrigation (Fig. 1-4). An important finding of this study was that 6 of 75 lesions had a sudden rise in electrical impedance associated with an audible pop. In these cases, the intramural temperature exceeded 100°C, resulting in sudden steam formation and a steam pop. The clinical concern about "pop lesions" is that sudden steam venting to the endocardial or epicardial surface (or both) can potentially cause perforation and tamponade.[20]

The observation of increasing lesion size with ablation-tip cooling holds true only so long as the ablation is not power limited. If a level of power is used that is insufficient to overcome the heat lost by convection, the resulting tissue heating may be inadequate. In this case, convective cooling will dissipate a greater proportion of energy, and less of the available RF energy will be converted into tissue heat. The resulting lesion may be smaller than it would be if there were no convective cooling. As power is increased to a higher level, more energy will be converted to tissue heat, and larger lesions will result. If power is unlimited and temperature feedback power control is employed, greater magnitudes of convective cooling will allow for higher power levels and very large lesions. Thus, paradoxically in this situation, lesion size may be inversely related to the electrode-tissue interface temperature if the ablation is not power limited.[21] However, if power level is fixed (most commercial RF generators limit power delivery to 50 W for use with these catheters), lesion size increases in proportion to electrode-tissue interface temperature even in the setting of significant convective cooling (Fig. 1-5).[22]

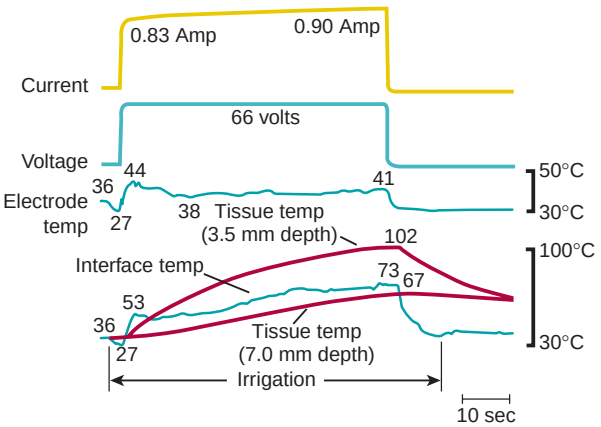

FIGURE 1-4. Current, voltage, and temperatures measured during radiofrequency catheter ablation with a perfused-tip electrode catheter in a canine exposed thigh muscle preparation are shown. Temperatures were recorded within the electrode, at the electrode-tissue interface, and within the muscle below the ablation catheter at depths of 3.5 and 7 mm. Because the electrode-tissue interface is actively cooled, high current and voltage levels can be employed. This results in an increased depth of direct resistive heating and superheating of the tissue below the surface of ablation. The peak temperature in this example at a depth of 3.5 mm was 102°C, and at 7 mm was 67°C, indicating that the 50°C isotherm defining the lesion border was significantly deeper than 7 mm. *(From Nakagawa H, Yamanashi WS, Pitha JV, et al. Comparison of in vivo tissue temperature profile and lesion geometry for radiofrequency ablation with a saline-irrigated electrode versus temperature control in a canine thigh muscle preparation.* Circulation. *1995;91:2264–2273. With permission.)*

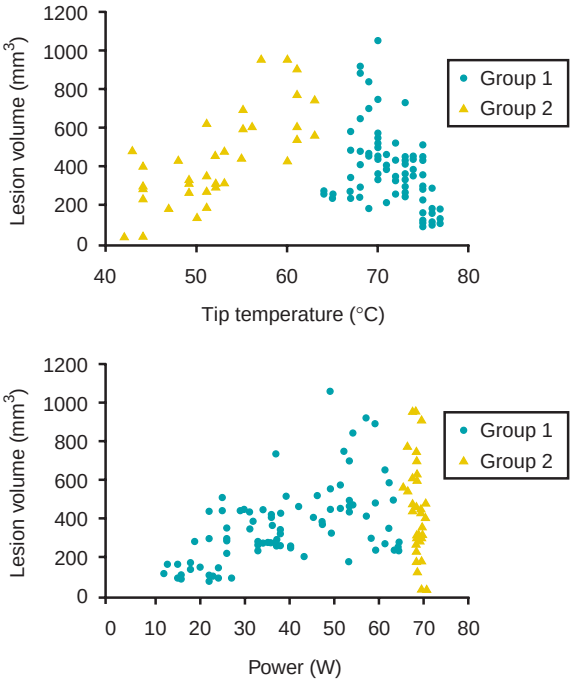

FIGURE 1-5. Temperatures measured at the tip of the electrode during experimental radiofrequency ablation and power are compared to the resulting lesion volume in this study. A maximal power of 70 W was employed. If lesion creation was not power limited (group 1), the lesion volume was a function of the delivered power. But if lesion production was limited by the 70-W available power maximum (group 2), the temperature measured at the electrode tip correlated with lesion size. *(From Petersen HH, Chen X, Pietersen A, et al. Lesion dimensions during temperature-controlled radiofrequency catheter ablation of left ventricular porcine myocardium: impact of ablation site, electrode size, and convective cooling.* Circulation. *1999;99:319–325. With permission.)*

ENDYMED EXHIBIT 1022 - 7/20

Electrode-tip cooling can be achieved passively or actively. Passive tip cooling occurs when the circulating blood flow cools the mass of the ablation electrode and cools the electrode-tissue interface. This can be enhanced by use of a large ablation electrode.[23] Active tip cooling can be realized with a closed or open perfused-tip system. In each case, circulating saline from an infusion pump actively cools the electrode tip. One design recirculates the saline through a return port, and the opposing design infuses the saline through weep holes in the electrode into the bloodstream. Both designs are effective and result in larger lesions and greater procedure efficacy than standard RF catheter ablation. Theoretical advantages and disadvantages of open perfusion versus closed perfusion catheter designs are claimed by device manufacturers and their spokespeople, but the lesions produced and the clinical efficacy and safety profiles of these competing designs are very comparable.[24–27] The tip cooling or perfusion has the apparent advantage of reducing the prevalence of coagulum and char formation. However, because the peak tissue temperature is shifted from the endocardial surface to deeper intramyocardial layers, there is the risk for excessive intramural heating and pop lesions. The challenge for the clinician lies with the fact that with varying degrees of convective cooling, there is no reliable method for monitoring whether tissue heating is inadequate, optimal, or excessive. Cooling at the electrode-tissue interface limits the value of temperature monitoring to prevent excess power delivery and steam pops. With closed irrigation catheters, there is some value in the use of temperature feedback power control. In this case, target temperatures of 42° to 45°C have been empirically determined to optimize energy delivery.[27,28] If the ablation is power limited and the target temperature has not been reached, one may assume that the combination of passive cooling (from sliding or bouncing catheter-tissue contact) and active cooling is dissipating too much energy to allow for adequate tissue heating. In this situation, active electrode cooling can be held, and the operator can depend on passive cooling alone.

Catheter orientation will affect lesion size and geometry. Perpendicular catheter orientation results in less electrode surface area in contact with the tissue and more surface area in contact with the circulating blood pool. Parallel catheter orientation provides more electrode-tissue contact. With unrestricted power delivery, the parallel orientation should produce the larger lesion. In perfused-tip catheters, parallel orientation also results in more active tissue cooling and smaller lesion sizes than a perpendicular orientation.[29] The resultant interplay among active cooling, passive cooling, and power availability or limitation determines whether the lesions will be larger or smaller in these varying conditions. If perfused-tip catheters are positioned in a parallel orientation with greater tissue cooling, the lesions are smaller in vitro because of diminished efficiency of energy delivery. The effects of catheter orientation are less important with 4- or 5-mm-tip catheters but become more dominant when 8- or 10-mm tips are employed.

Since its inception, conventional RF ablation has been characterized by its excellent safety profile. This undoubtedly has been due to the relatively small size of the lesions. As new catheter technologies designed to increase the depth of the ablative lesion have been employed, it is not surprising that complications due to collateral injury have increased. For example, left atrial ablation with cooled ablation catheters and high-intensity, focused ultrasound has resulted in cases of esophageal injury, perforation, and death. Despite the routine positioning of ablation catheters in close proximity to coronary arteries, there has been a dearth of coronary arterial complications with this procedure. The blood flow within the coronary artery is rapid, and the zone of tissue around the artery is convectively cooled by this blood flow. Fuller and Wood tested the effect of flow rate through a marginal artery of Langendorff perfused rabbit hearts.[30] RF ablation with an electrode-tissue interface temperature of 60° or 80°C was performed on the right ventricular free wall with two lesions straddling the artery, and conduction through this region was monitored. They observed that arterial flow rates as low as 1 mL/minute through these small (0.34 ± 0.1 mm diameter) arteries prevented complete transmural ablation and conduction block. This heat-sink effect is especially protective of the vascular endothelium. With higher power output of new ablation technologies, however, the convective cooling of the arterial flow may be overwhelmed, and there may be increased risk for vascular injury. With greater destructive power possible, operators need to be mindful to use only enough power to achieve complete ablation of the targeted tissue in order to safely accomplish the goal of arrhythmia ablation.

Electrical Current Distribution

Catheter ablation depends on the passage of RF electrical current through tissue. Tissue contact can be assessed by measuring baseline system impedance. In one clinical study, a very small (10 μA) current was passed through the ablation catheter, and the efficiency of heating was measured to assess tissue contact. A significant positive correlation between preablation impedance and heating efficiency was observed. As tissue is heated, there is a temperature-dependent fall in the electrical impedance.[31,32] A significant correlation is also observed between heating efficiency and the maximal drop in impedance during energy delivery. When electrode-tissue interface temperature monitoring is unreliable because of high-magnitude convective cooling, the slow impedance drop is a useful indicator that tissue heating is occurring. With the progressive fall in impedance during ablation, the delivered current increases along with tissue heating. If no impedance drop is observed, catheter repositioning is warranted.[33,34]

Because the magnitude of tissue heating is determined by the current density, the distribution of RF field around the electrodes in unipolar, bipolar, or phased RF energy delivery will determine the distribution of tissue heating. If energy is delivered in a unipolar fashion in a uniform medium from a spherical electrode to an indifferent electrode with infinite surface area, current density around the electrode should be entirely uniform. As geometries and tissue properties change, heating becomes nonuniform. Standard 4-mm electrode tips are small enough so that heating around the tip is fairly evenly distributed, even with varying tip contact angle to the tissue. One study showed that temperature monitoring with a thermistor located at the tip of a 4-mm electrode underestimated the peak electrode-tissue interface temperature recorded from multiple temperature

ENDYMED EXHIBIT 1022 - 8/20

ENDYMED EXHIBIT 1022 - 9/20

sensors distributed around the electrode in only 4% of the applications. In RF applications where high power was employed and a sudden rise in electrical impedance occurred, the peak temperature recorded from the electrode tip was below 95°C in only one of 17 cases.[35] However, present-day electrode geometries vary considerably. The presence of fat will alter both electrical and thermal conductivity. Epicardial ablation over fat will result in minimal ablation of the underlying myocardium. Conversely, ablation of tissue insulated by fat outside of the ablation target will produce an "oven" effect, with higher temperatures for longer durations after cessation of energy delivery.[36] Also, tissue characteristics and placements of indifferent electrodes will affect tissue heating. Surface temperature recordings routinely underestimate peak subendocardial tissue temperatures. For that reason, most operators limit ablation temperatures to 60° or 70°C during ablation with noncooled catheters.

Dispersive Electrode

The power dissipated in the complete circuit is proportional to the voltage drop and impedance for each part of the series circuit. The impedance of the ablation system and transmission lines is low, so there is little energy dissipation outside the body. The site of greatest impedance, voltage drop, and power dissipation is at the electrode-tissue interface (Fig. 1-6). However, most power is consumed with electrical conduction through the body and blood pool and into the dispersive electrode. In fact, only a fraction of the total delivered power actually is deposited in

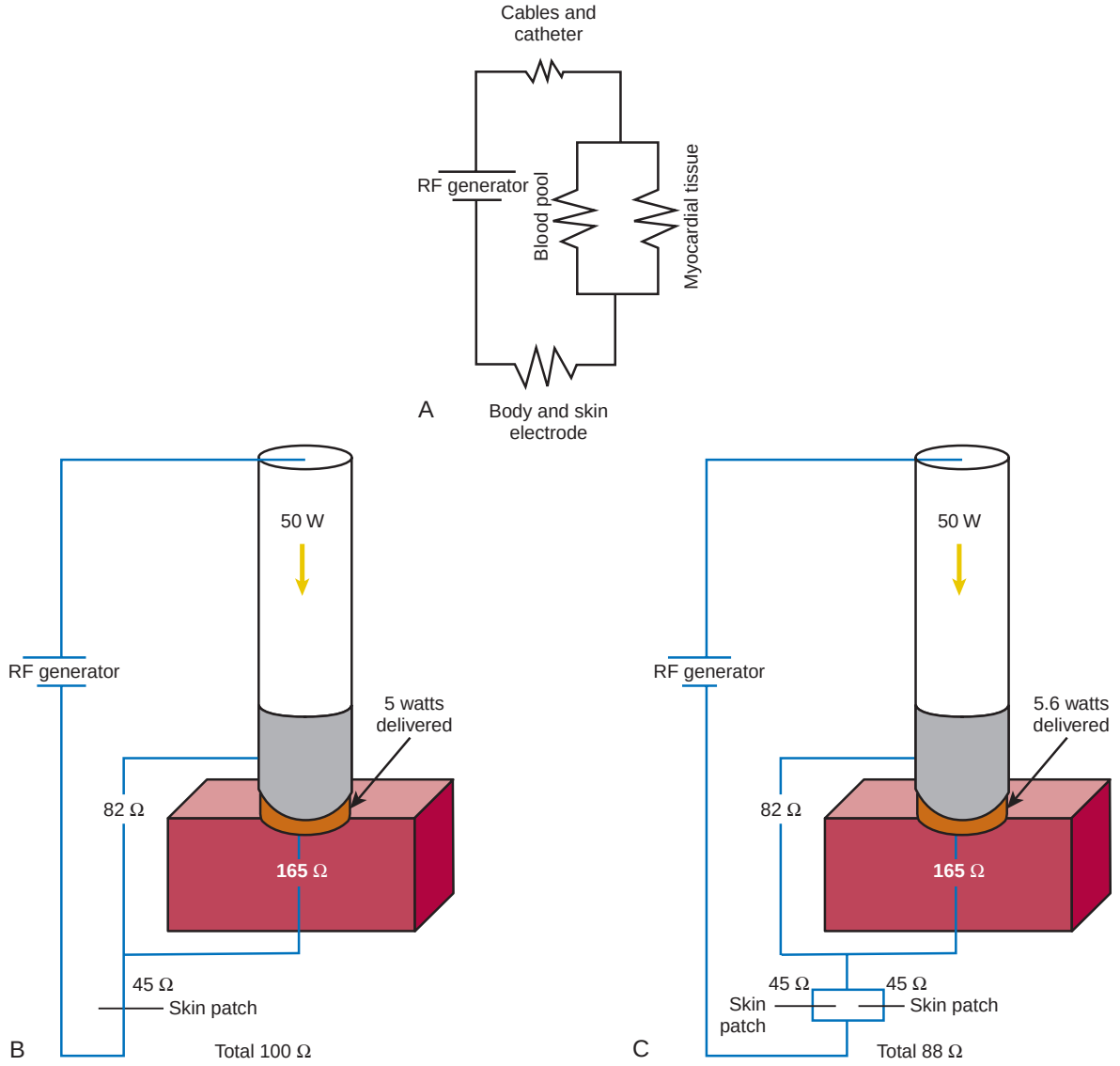

FIGURE 1-6. "Circuit diagrams" for radiofrequency (RF) ablation. **A,** From the RF generator, the cables and catheter present minimal resistance. The myocardial tissue and blood pool represent resistance circuits in parallel from the distal electrode. The return path from the ablation electrode to the generator comprises the patient's body and dispersive electrode in series. **B,** Hypothetical resistances for RF ablation circuit path. The resistance of the blood pool is about half that of the myocardial tissue. In this situation, for 50 W of energy delivered to the catheter, only 5 W is deposited in the myocardial tissue because of shunting of current through the lower resistance blood pool and power loss in the return path. **C,** Effect of adding a second dispersive skin electrode to the circuit. Assuming that the impedance of each dispersive electrode is 45 ohms and the generator voltage is constant, the total ablation circuit impedance is decreased by 12%. This allows for greater current delivery through the circuit and a proportional increase in power delivered to the tissue.

the myocardial tissue (Fig. 1-6). The return path of current to the indifferent electrode will certainly affect the current density close to that indifferent electrode, but its placement anterior versus posterior, and high versus low on the torso, has only a small effect on the distribution of RF current field lines within millimeters of the electrode. Therefore, lesion geometry should not be affected greatly by dispersive electrode placement. However, the proportion of RF energy contributing to lesion formation will be reduced if a greater proportion of that energy is dissipated in a long return pathway to the dispersive electrode. When the ablation is power limited, it is advantageous to minimize the proportion of energy that is dissipated along the current pathway at sites other than the electrode-tissue interface to achieve the greatest magnitude of tissue heating and the largest lesion. In an experiment that tested placement of the dispersive electrode directly opposite the ablation electrode versus at a more remote site, lesion depth was increased 26% with optimal placement.[37] Vigorous skin preparation to minimize impedance at the skin interface with the dispersive electrode, closer placement of the dispersive electrode to the heart, and use of multiple dispersive electrodes to increase skin contact area will all increase tissue heating in a power-limited energy delivery. Nath and associates reported that in the setting of a system impedance higher than 100 ohms, adding a second dispersive electrode increased the peak electrode-tip temperature during clinical catheter ablation (Fig. 1-7).[38]

Edge Effect

Electrical field lines are not entirely uniform around the tip of a unipolar ablation electrode. The distribution of field lines from an electrode source is affected by changes in electrode geometry. At points of geometric transition, the field lines become more concentrated. This so-called edge effect can result in significant nonuniformity of heating around electrodes. The less symmetrical the electrode design (such as if found with long electrodes), the greater the degree of nonuniform heating. McRury and coworkers tested ablation with electrodes with 12.5-mm length.[39] They found that a centrally placed temperature sensor significantly underestimated the peak electrode-tissue interface temperature. Finite element analysis demonstrated a concentration of electrical current at the each of the electrode edges (Fig. 1-8). When dual thermocouples were placed on the edge of the electrode, the risk for coagulum formation and impedance rise was significantly reduced during ablation testing in vivo.

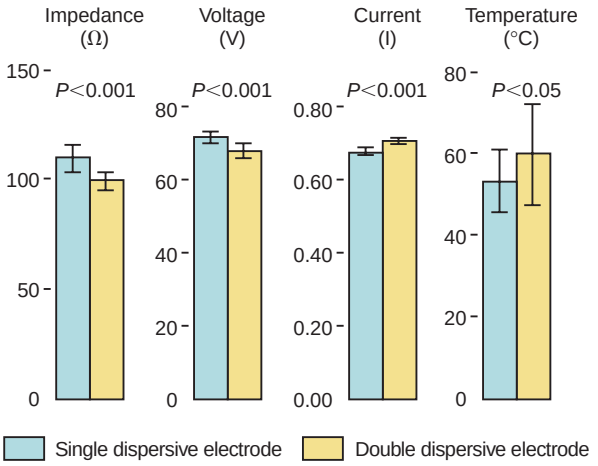

FIGURE 1-7. Impedance, voltage, current, and catheter-tip temperature readings during radiofrequency catheter ablation in a subset of patients with a baseline system impedance of more than 100 ohms. Ablations using a single dispersive electrode were compared with those using a double dispersive electrode. A lower system impedance was observed with addition of the second dispersive patch. This resulted in a greater current delivery and higher temperatures measured at the electrode-tissue interface. *(From Nath S, DiMarco JP, Gallop RG, et al. Effects of dispersive electrode position and surface area on electrical parameters and temperature during radiofrequency catheter ablation.* Am J Cardiol. *1996;77:765–767. With permission.)*

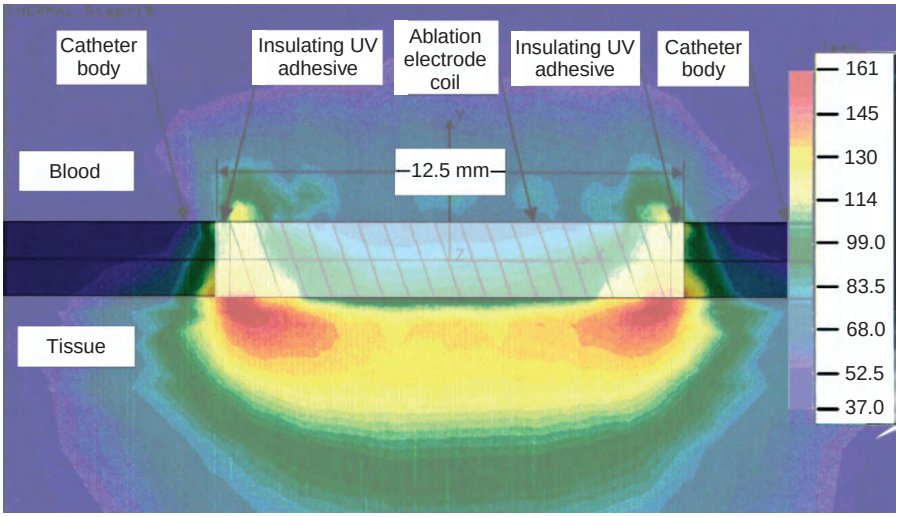

FIGURE 1-8. Steady-state temperature distribution derived from a finite element analysis of radiofrequency ablation with a 12-mm long coil electrode. In this analysis, the electrode temperature at the center of the electrode was maintained at 71°C. The legend of temperatures is shown at the right of the graph and ranges from the physiologic normal (violet = 37°C) to the maximal tissue temperature (red = 161°C) located below the electrode edges. There is a significant gradient of heating between the peak temperatures at the electrode edges and the center of the electrode. UV, ultraviolet. *(From McRury ID, Panescu D, Mitchell MA, Haines DE. Nonuniform heating during radiofrequency catheter ablation with long electrodes: monitoring the edge effect.* Circulation. *1997;96:4057–4064. With permission.)*

ENDYMED EXHIBIT 1022 - 10/20

Tissue Pathology and Pathophysiologic Response to Radiofrequency Ablation

Gross Pathology and Histopathology of the Ablative Lesion

The endocardial surface in contact with the ablation catheter shows pallor and sometimes a small depression due to volume loss of the acute lesion. If excessive power has been applied, there may be visible coagulum or char adherent to the ablation site. On sectioning the acute lesion produced by RF energy, a central zone of pallor and tissue desiccation characterizes its gross appearance. There is volume loss, and the lesion frequently has a teardrop shape with a narrower lesion width immediately subendocardially and a wider width 2 to 3 mm below the endocardial surface. This is because of surface convective cooling by the endocardial blood flow. Immediately outside the pale central zone is a band of hemorrhagic tissue. Beyond that border, the tissue appears relatively normal. The acute lesion border, as assessed by vital staining, correlates with the border between the hemorrhagic and normal tissue (Fig. 1-9). The histologic appearance of the lesion is consistent with coagulation necrosis. There are contraction bands in the sarcomeres, nuclear pyknosis, and basophilic stippling consistent with intracellular calcium overload.[40]

The temperature at the border zone of an acute hyperthermic lesion assessed by vital staining with nitro blue tetrazolium is 52° to 55°C.[3] However, it is likely that the actual isotherm of irreversible thermal injury occurs at a lower temperature boundary outside the lesion boundary, but that it cannot be identified acutely. Coagulation necrosis is a manifestation of thermal inactivation of the contractile and cytoskeletal proteins in the cell. Changes in the appearance of vital stains are due to loss of enzyme activity, as is the case with nitro blue tetrazolium staining and dehydrogenase activity.[41] Therefore, the acute assessment of the lesion border represents the border of thermal inactivation of various proteins, but the ultimate viability of the cell may depend on the integrity of more thermally sensitive organelles such as the plasma membrane (see later). In the clinical setting, recorded temperature does correlate with response to ablation. In patients with manifest Wolff-Parkinson-White syndrome, reversible accessory pathway conduction block was observed at a mean electrode temperature of 50° ± 8°C, whereas permanent block occurred at a temperature of 62° ± 15°C.[42] In a study of electrode-tip temperature monitoring during atrioventricular junctional ablation, an accelerated junctional rhythm was observed at a mean temperature of 51° ± 4°C. Permanent complete heart block was observed at ablation temperatures of 60° ± 7°C.[43] Because the targeted tissue was likely millimeters below the endocardial surface, the temperatures recorded by the catheter were likely higher than those achieved intramurally at the critical site of ablation.

The subacute pathology of the RF lesion is similar to what is observed with other types of injury. The appearance of typical coagulation necrosis persists, but the lesion border becomes more sharply demarcated with infiltration of mononuclear inflammatory cells. A layer of fibrin adheres to the lesion surface, coating the area of endothelial injury.

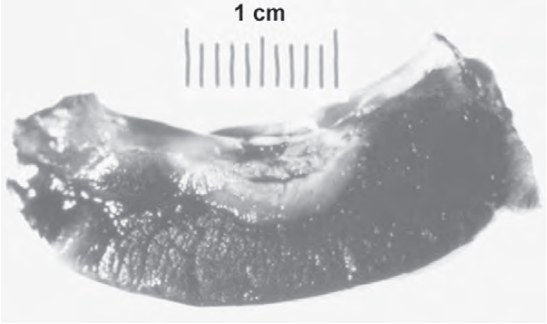

FIGURE 1-9. Typical appearance of radiofrequency catheter ablation lesion. There is a small central depression with volume loss, surrounded by an area of pallor, then a hemorrhagic border zone. The specimen has been stained with nitro blue tetrazolium to differentiate viable from nonviable tissue.

After 4 to 5 days, the transition zone at the lesion border is lost, and the border between the RF lesion and surrounding tissue becomes sharply demarcated. The changes in the transition zone within the first hours and days after ablation likely account for the phenomena of early arrhythmia recurrence (injury with recovery)[44] or delayed cure (progressive injury due to the secondary inflammatory response).[45] The coagulation necrosis in the body of the lesion shows early evidence of fatty infiltration. By 8 weeks after ablation, the necrotic zone is replaced with fatty tissue, cartilage, and fibrosis and can be surrounded by chronic inflammation.[46] The chronic RF ablative lesion evolves to uniform scar. The uniformity of the healed lesion accounts for the absence of any proarrhythmic effect of RF catheter ablation, unless multiple lesions with gaps are made. Like any fibrotic scar, there is significant contraction of the scar with healing. Relatively large and wide acute linear lesions have the final gross appearance of narrow lines of glistening scar when examined 6 months after the ablation procedure.[47]

Radiofrequency Lesion Ultrastructure

The ultrastructural appearance of the acute RF lesion offers some insight into the mechanism of tissue injury at the lesion border zone. In cases of experimental RF ablation in vivo, ventricular myocardium was examined in a band 3 mm from the edge of the acute pathologic lesion as defined by vital staining (Fig. 1-10). It showed marked disruption in cellular architecture characterized by dissolution of lipid membranes and inactivation of structural proteins. The plasma membranes were severely disrupted or missing. There was extravasation of erythrocytes and complete absence of basement membrane. The mitochondria showed marked distortion of architecture with swollen and discontinuous cristae membranes. The sarcomeres were extended with loss of myofilament structure or were severely contracted. The T-tubules and sarcoplasmic reticulum were absent or severely disrupted. Gap junctions were severely distorted or absent. Thus, despite the fact that the tissue examined was outside of the border of the acute pathologic lesion, the changes were profound enough to conclude that some progression of necrosis would occur within this border zone. The band of tissue 3 to 6 mm from the edge of the pathologic lesion was examined and manifested significant ultrastructural

ENDYMED EXHIBIT 1022 - 11/20

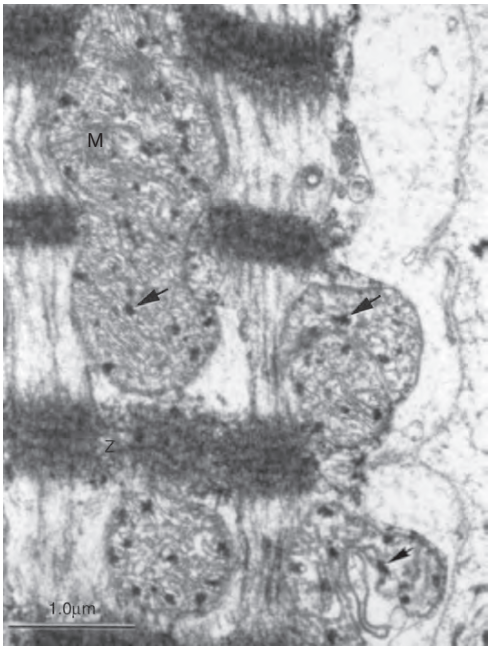

FIGURE 1-10. Electron micrograph of a myocardial sample 3 mm outside of the border zone of acute injury created by radiofrequency catheter ablation. There is severe disruption of the sarcomere with contracted Z bands, disorganized mitochondria, and basophilic stippling (*arrows*). Bar scale is 1.0 µm. *(From Nath S, Redick JA, Whayne JG, Haines DE. Ultrastructural observations in the myocardium beyond the region of acute coagulation necrosis following radiofrequency catheter ablation.* J Cardiovasc Electrophysiol. *1994;5:838–845. With permission.)*

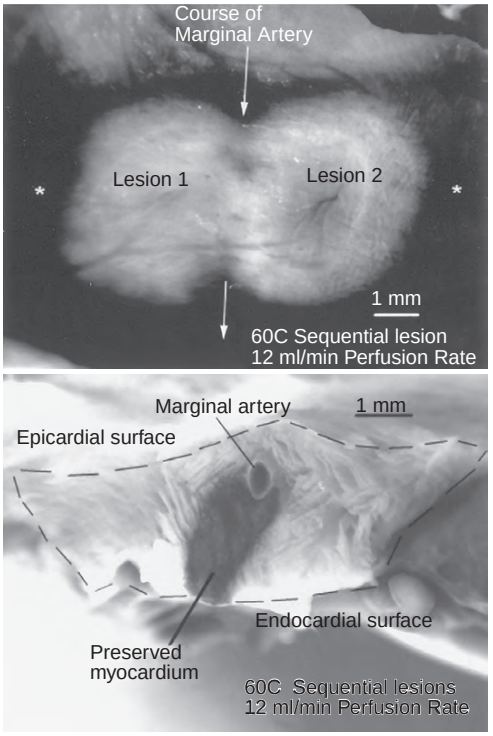

FIGURE 1-11. Top, Epicardial view of two radiofrequency lesions created during perfusion of a penetrating marginal artery in a rabbit heart. The lesions show central pallor that is apparent after vital staining. The course of the artery is marked. The *asterisks* mark the line used for perpendicular sectioning of the lesion. **Bottom,** Cross section through the middle of lesion perpendicular to marginal artery. The *broken lines* outline the lesion boundary. A region of myocardial sparing contiguous to the penetrating marginal artery (labeled) is apparent. Electrical conduction was present across this bridge of viable myocardium post ablation. *(From Fuller LA, Wood MA: Intramural coronary vasculature prevents transmural radiofrequency lesion formation: implications for linear ablation.* Circulation. *2003;107:1797–1803. With permission.)*

abnormalities, but not as severe as those described closer to the lesion core. Severe abnormalities of the plasma membrane were still present, but gap junctions and mitochondria were mainly intact. The sarcomeres were variable in appearance, with some relatively normal and some partially contracted. Although ultrastructural disarray was observed in the 3- to 6-mm zone, the myocytes appeared to be viable and would likely recover from the injury.[48]

Radiofrequency Ablation and Arterial Perfusion

In addition to direct injury to the myocytes, RF-induced hyperthermia has an effect on the myocardial vasculature and the myocardial perfusion. Impairment of the microcirculation could contribute to lesion formation by an ischemic mechanism. A study examined the effects of microvascular perfusion during acute RF lesion formation. In open chest canine preparations, the left ventricle was imaged with ultrasound from the epicardial surface, and a myocardial echocardiographic contrast agent was injected into the left anterior descending artery during endocardial RF catheter ablation. After ablation, the center of the lesion showed no echo contrast, consistent with severe vascular injury and absence of blood flow to that region. In the border zone of the lesion, a halo effect of retained myocardial contrast was observed. This suggested marked slowing of contrast transit rate through these tissues. The measured contrast transit rate at the boundary of the gross pathologic lesion was 25% ± 12% of the transit rate in normal tissue. In the 3-mm band of myocardium outside of the lesion edge, the contrast transit was 48% ± 27% of normal, and in the band of myocardium 3 to 6 mm outside of the lesion edge, the transit rate was 82% ± 28% of normal ($P < .05$ for all comparisons). The ultrastructural appearance of the arterioles demonstrated marked disruption of the plasma membrane and basement membrane and extravasation of red blood cells in these regions of impaired myocardial perfusion. The relative contribution of microvascular injury and myocardial ischemia to ultimate lesion formation is unknown but may play a role in lesion extension during the early phases after ablation.[49]

The effect of RF heating on larger arteries is a function of the size of the artery, the arterial flow rate, and the proximity to the RF source. In one study, flow rate through a marginal artery (or intramural perfusion cannula) in an in vitro rabbit heart preparation was varied between 0 and 10 mL/minute. A pair of epicardial ablations was produced with epicardial RF energy applications. Even at low flow rates, there was substantial sparing of the artery and the surrounding tissue owing to the heat-sink effect of the arterial flow (Fig. 1-11). However, if 45 W of power was applied along with RF electrode-tip cooling, complete ablation of the tissue contiguous to the intramural

perfusion cannula was achieved.[30] Although this may be a desirable effect in the setting of small perfusing arteries through a region of conduction critical for arrhythmia propagation, it is not desirable if the artery is a large epicardial artery that happens to be contiguous to an ablation site, as is sometimes the case with accessory pathway or slow atrioventricular nodal pathway ablation, or ablation in the tricuspid-subeustachian isthmus for atrial flutter. Cases of arterial injury have been reported, particularly with the use of large-tip or tip-cooling technologies that allow for application of high RF powers.[50,51] In particular, when high-power ablation is required within the coronary sinus or great cardiac vein, it is prudent to define the course of the arterial anatomy to avoid unwanted arterial thermal injury.

Collateral Injury from Ablation

The injury to targeted myocardium is usually achieved if effort is made to optimize electrode-tissue contact. To ensure procedural success, particularly with ablation of more complex substrates like those found with atrial fibrillation, operators have employed a number of large-lesion RF technologies such as cooled-tip, perfused-tip, or large-tip catheters. With deep lesions sometimes comes unintended collateral injury to contiguous structures. An understanding of the anatomic relationships and careful titration of RF energy delivery can avoid adverse consequences of ablation in most cases. A rare but dangerous complication of ablation of the posterior left atrium is esophageal injury, often leading to atrioesophageal fistula or esophageal perforation.[52] The esophagus is located immediately contiguous to the atrium in most patients, with a distance from atrial endocardium to esophagus as small as 1.6 mm.[53] Hyperthermic injury leads to damage to structural proteins resulting in significant reduction in tensile strength of the esophageal musculature.[54] That, coupled with esophageal mucosal injury and ulcer formation, likely leads to ultimate perforation with a high case-fatality rate. Other structures that can be damaged with pulmonary vein isolation procedures are vagal and phrenic nerves.[55,56] Although these nerves usually regenerate after several months, permanent palsy can occur. Avoiding injury to these structures while achieving reliable transmural ablation of the myocardium can be challenging. Power should be limited, heating should be monitored carefully with multiple modalities (temperature, impedance drop, microbubbles on intracardiac echocardiogram imaging), and duration of energy delivery should be kept to a minimum. A complication of ablation of atrial fibrillation that was prevalent when ablation was being performed within the vein was pulmonary vein stenosis.[57] If the temperature rise of the venous wall is excessive, irreversible changes in the collagen and elastin of the vein wall will occur. In vitro heating of pulmonary vein rings showed a 53% reduction in circumference and a loss of compliance with hyperthermic exposure at or above 70°C. After exposure to those temperatures, the histologic examination showed loss of the typical collagen structure, presumably due to thermal denaturation of that protein.[58] For this reason, most pulmonary vein isolation is now performed outside the vein in the pulmonary vein antrum.

Cellular Mechanisms of Thermal Injury

The therapeutic effect of RF catheter ablation is due to electrical heating of tissue and thermal injury. The field of hyperthermia is broad, and the effects of long-duration exposures to mild and moderate hyperthermia have been well characterized in the oncology literature. Thermal injury is dependent upon both time and temperature. For example, when human bone marrow cells in culture are exposed to a temperature of 42°C, cell survival is 45% at 300 minutes. But when those cells are heated to 45.5°C, survival at 20 minutes is only 1%.[59] Data regarding the effects of brief exposure of myocardium to higher temperatures, as is the case during catheter ablation, is more limited and is reviewed in this section. The central zone of the ablation lesion reaches high temperatures and is simply coagulated. Lower temperatures are reached during the ablation in the border zones of the lesion. The responses of the various cellular components to low and moderate hyperthermia determine the pathophysiologic response to ablation. The thermally sensitive elements that contribute to overall thermal injury to the myocyte include the plasma membrane with its integrated channel proteins, the nucleus, and the cytoskeleton. Changes in these structures that occur during hyperthermic exposure all contribute to the ultimate demise of the cell.

Plasma Membrane

The plasma membrane is very thermally sensitive. A pure phospholipid bilayer will undergo phase transitions from a relatively solid form to a semiliquid form. Addition of integral proteins and the varying composition of the phospholipids with regard to the saturation of the hydrocarbon side chains affect the degree of membrane fluidity in eukaryotic cells. In one study, cultured mammalian cell membranes were found to have a phase transition at 8°C, and a second transition between 22° and 36°C. No phase changes were seen in the 37° to 45°C temperature range, but studies have not been performed examining this phenomenon in sarcomeres, or at temperatures above 45°C.[60] Regarding the function of integral plasma membrane proteins during exposure to heating, both inhibition and accentuation of protein activity have been observed. Stevenson and colleagues reported an increase in intracellular K^+ uptake in cultured Chinese hamster ovary (CHO) cells during heating to 42°C. This was blocked by ouabain, indicating an increased activity of the Na^+,K^+-ATPase pump.[61] Nath and colleagues examined action potentials in vitro in a superfused guinea pig papillary muscle preparation. In the low hyperthermic range between 38° and 45°C, there was an increase in the maximal dV/dt of the action potential, indicating enhanced sodium channel kinetics. In the moderate hyperthermia range from 45° to 50°C, the maximal dV/dt decreased below baseline values. The mechanism of this sodium channel inhibition was hypothesized to be either partial thermal inactivation of the sodium channel or, more likely, voltage-dependent sodium channel inactivation due to thermally mediated cellular depolarization[62] (see later).

ENDYMED EXHIBIT 1022 - 13/20

Cytoskeleton

The cytoskeleton is composed of structural proteins that form microtubules, microfilaments, and intermediate filaments. The microfilaments coalesce into stress filaments. These include the proteins actin, actinin, and tropomyosin and form the framework to which the contractile elements of the myocyte attach. The cytoskeletal elements may have varying degrees of thermal sensitivity depending on the cell type. For example, in human erythrocytes, the cytoskeleton is composed predominantly of the protein spectrin. Spectrin is thermally inactivated at 50°C. When erythrocytes are exposed to temperatures above 50°C, the erythrocytes rapidly lose their biconcave shape.[63] There is no scientific literature reporting the inactivation temperature of the cytoskeletal proteins in myocytes. However, electron micrographs of the border zone of RF lesions show significant disruption in the cellular architecture with loss of the myofilament structure.[48] In the central portion of the RF lesion, thermal inactivation of the cytoskeleton contributes to the typical appearance of coagulation necrosis.

Nucleus

The eukaryote nucleus shows evidence of thermal sensitivity in both structure and function. Nuclear membrane vesiculation, condensation of cytoplasmic elements in the perinuclear region, and a decrease in heterochromatin content have been described.[64,65] The nucleolus appears to be the most heat-sensitive component of the nucleus. Whether or not hyperthermia induces DNA strand breaks is controversial. One reproducible finding after hyperthermic exposure is the elaboration of nuclear proteins called *heat shock proteins*. The function of heat shock proteins has not been entirely elucidated, but they appear to exert a protective effect on the cell. It is hypothesized that HSP 70 facilitates the effective production and folding of proteins and assists their transit among organelles.[66]

Cellular Electrophysiology

Hyperthermia leads to dramatic effects on the electrophysiology of myocardium. The thermal sensitivity of myocytes has been tested in a variety of experimental systems, and the mechanisms of the electrophysiologic responses to catheter ablation have been elucidated. In one series of in vitro experiments, isolated superfused guinea pig papillary muscles were subjected to 60 seconds of exposure to hyperthermic superfusate at temperatures varying from 38° to 55°C. Action potentials were recorded continuously during and after the hyperthermic pulse. If resting membrane potential was not restored after return to normothermia, the muscle was discarded, and testing proceeded with a new tissue sample. The resting membrane potential was assessed in unpaced preparations, and the action potential amplitude, duration, dV/dt, and excitability were tested during pacing. The preparations maintained a normal resting membrane potential in the low hyperthermic range (<45°C). In the intermediate hyperthermic range (45° to 50°C), the myocytes showed a temperature-dependent depolarization that was reversible on return to normothermic superfusion. Finally, experiments in the high hyperthermic range (>50°C) typically resulted in irreversible depolarization, contracture, and death

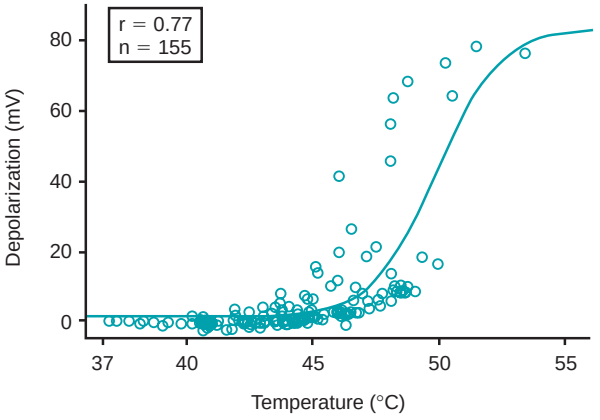

FIGURE 1-12. The magnitude of depolarization of guinea pig papillary muscle cells exposed to 1-minute pulses of hyperthermic perfusate versus perfusate temperature. At temperatures below 45°C, little depolarization is seen. The cells have progressive depolarization between 45° and 50°C. Above 50°C, few recordings are made because most cells have irreversible contracture and death. *(From Nath S, Lynch C III, Whayne JG, Haines DE. Cellular electrophysiological effects of hyperthermia on isolated guinea pig papillary muscle: implications for catheter ablation.* Circulation. *1993;88:1826–1831. With permission.)*

(Fig. 1-12). There was a temperature-dependent decrease in action potential amplitude between 37° and 50°C as well as an inverse linear relationship between temperature and action potential duration. With increasing temperatures, the dV/dt increased, but above 46°C this measurement began to decrease in preparations that had a greater magnitude of resting membrane potential depolarization. Spontaneous automaticity was observed in both paced and unpaced preparations at a median temperature of 50°C, compared with a temperature of 44°C in preparations without automaticity. The occurrence of automaticity in unpaced preparations in the setting of hyperthermia-induced depolarization suggested abnormal automaticity as the mechanism. Beginning at temperatures higher than 42°C, loss of excitability to external-field stimulation was seen in some paced preparations and was dependent on the resting membrane potential. Mean resting membrane potential observed with loss of excitability was −44 mV, compared with −82 mV for normal excitability. The superfusate temperature measured during reversible loss of excitability was 43° to 51°C, but irreversible loss of excitability (cell death) occurred only at temperatures of 50°C or higher.[62] Thus, it appeared from these experiments that there was increased cationic entry into the hyperthermic cell and that the resultant depolarization led to loss of excitability and cell death.

Calcium Overload and Cellular Injury

In a preparation similar to that described previously, Everett and colleagues further elucidated the specific mechanisms for cellular depolarization and death in response to hyperthermia.[67] Isolated superfused guinea pig papillary muscles were attached to a force transducer to assess the pattern of contractility with varying hyperthermic exposure. Consistent with the observations of resting membrane potential changes during heating, there was a reversible increase in tonic resting muscle tension at temperatures between 45° and 50°C. Above 50°C, the preparations showed evidence of

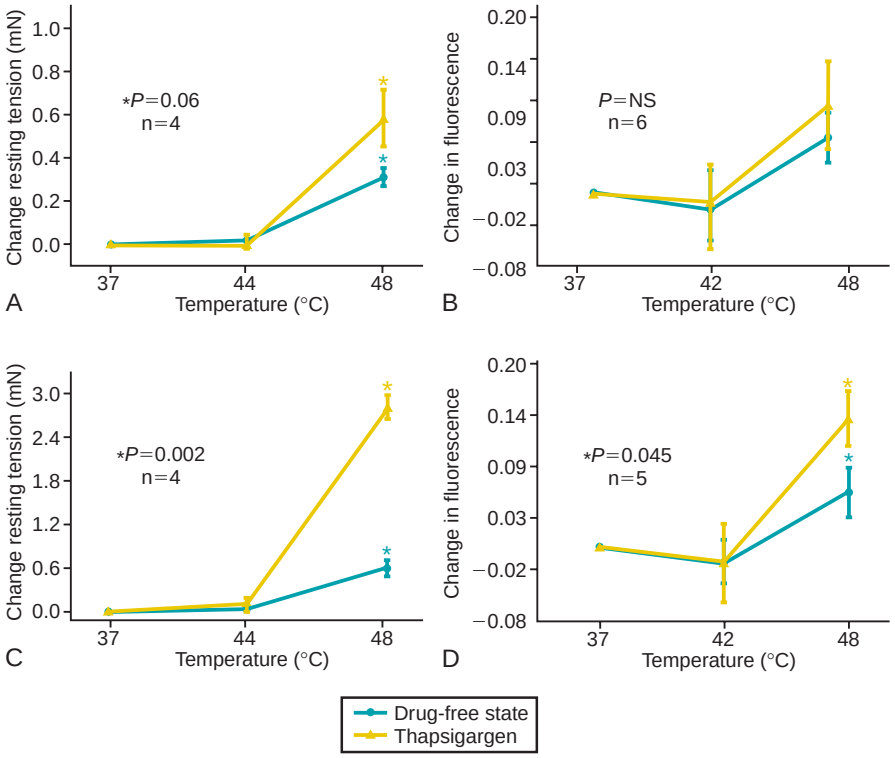

FIGURE 1-13. The effects of hyperthermic exposure on calcium entry into cells was tested in isolated perfused guinea pig papillary muscles. A change in resting tension was used as a surrogate measure for cytosolic calcium concentration (**A, C**), and a change in Fluo-3 AM fluorescence was used as a direct measure of free cytosolic calcium (**B, D**). With exposure to mild hyperthermia (42° to 44°C), little change in calcium levels was observed. With moderate hyperthermia (48°C), however, muscle tension and Fluo-3 AM fluorescence increased significantly. This increase was not channel specific because calcium channel blockade with cadmium or verapamil did not alter this response (**A, B**). The response was accentuated by thapsigargin (**C, D**), an agent that blocks calcium reuptake by the sarcoplasmic reticulum. *(From Everett TH, Nath S, Lynch C III, et al. Role of calcium in acute hyperthermic myocardial injury.* J Cardiovasc Electrophysiol. *2001;12:563–569. With permission.)*

irreversible contracture. This suggested that hyperthermia was causing calcium entry into the cell and ultimately calcium overload. This hypothesis was confirmed with calcium-sensitive Fluo-3 AM dye. Hyperthermic increases in papillary muscle tension correlated well with Fluo-3 AM luminescence. To elucidate the mechanism of calcium entry into the cell and its role in cellular injury, preparations were pretreated with either a calcium channel blocker (cadmium or verapamil) or an inhibitor of the sarcoplasmic reticulum calcium pump (thapsigargin). Preparations heated to 42° to 44°C showed no significant changes in tension at baseline or with drug treatment. With exposure to 48°C, treatment with calcium channel blockers did not reduce the increase in resting tension or Fluo-3 AM fluorescence, suggesting that the increase in cytosolic calcium was not the consequence of channel-specific calcium entry into the cell. In contrast, thapsigargin treatment led to irreversible papillary muscle contracture at lower temperatures (45% to 50°C) than observed without this agent. For preparations heated to 48°C, there was a greater increase in muscle tension and Fluo-3 AM fluorescence in the thapsigargin group compared with controls (Fig. 1-13). The authors concluded that hyperthermia results in significant increases in intracellular calcium, probably as a result of nonspecific transmembrane transit through thermally induced sarcolemmal pores. With increased intracellular calcium entry, the sarcoplasmic reticulum acts as a protective buffer against calcium overload, unless this function is blocked with an agent like thapsigargin. In this case, cell contracture and death occur at lower temperatures than expected.[67]

Conduction Velocity

Simmers and coworkers have examined the effects of hyperthermia on impulse conduction in vitro in a preparation of superfused canine myocardium.[68] Average conduction velocity at baseline temperatures of 37°C was 0.35 m/second. When the superfusate temperature was raised, conduction velocity increased to supernormal values, reaching a maximum of 114% of baseline at 42.5°C. At temperatures above 45.4°C, conduction velocity slowed. Transient conduction block was observed between 49.5° and 51.5°C, and above 51.7°C permanent block was observed (Fig. 1-14).[68] These findings are exactly concordant with the temperature-related changes in cellular electrophysiology described previously. In a related experiment, the authors assessed myocardial conduction across a surgically created isthmus during heating with RF energy. The temperatures recorded during transient conduction block (50.7° ± 3.0°C) and permanent conduction block (58.0° ± 3.4°C) were nearly identical to those temperature ranges recorded in the experiments performed with hyperthermic perfusate. The authors concluded that the sole effects of RF ablation on the electrophysiologic properties of the myocardium were hyperthermic, and that there was no

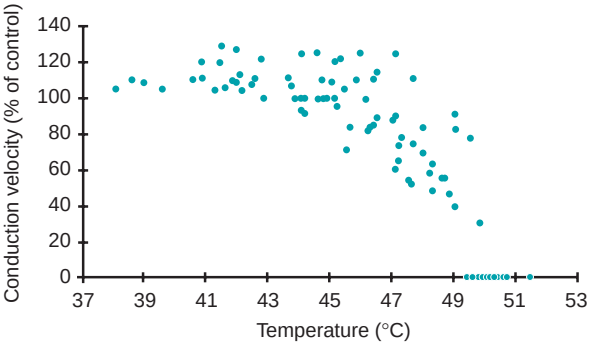

FIGURE 1-14. Conduction velocity of myocardium in superfused canine myocardium in vitro versus the temperature of the superfusate. A mild augmentation of conduction velocity due to an increase in dV/dt is observed at temperatures up to 45°C. Between 45° and 50°C, conduction velocity falls, and above 50°C, conduction is blocked. *(From Simmers TA, de Bakker JM, Wittkampf FH, Hauer RN. Effects of heating on impulse propagation in superfused canine myocardium.* J Am Coll Cardiol. *1995;25:1457–1464. With permission.)*

additional pathophysiologic response that could be attributed to direct effects of passage of electrical current through the tissue.[69] It is unknown whether these changes in conduction velocity are due solely to changes in intracellular ionic concentrations or whether thermal injury to gap junctions may also be implicated.

Determinants of Lesion Size

Targeting

The success of catheter ablation is dependent on a several factors. The first and foremost factor is optimizing targeting of the arrhythmogenic substrate. It is intuitive that increasing the size and depth of an ablative lesion will not improve the ablation success if the site selected for ablation is poor. To optimize site selection, it is necessary to understand the physiology and the anatomy of the arrhythmia in its entirety. The proximity of the electrode to the target will be the most important factor for ablation success.

Tissue Composition

Lesion sizes are decreased in areas of dense scar. In addition, an insulating layer of fat as thin as 2 mm overlying myocardial tissue (as in epicardial ablation) will prevent formation of a lesion with RF energy delivery.[70]

Power

Lesion size is proportional to power. Any method that will allow for greater power deposition into the tissue will result in more tissue heating and greater depth of thermal injury. In addition to power amplitude, efficiency of power coupling to the tissue (i.e., how much power is converted to tissue heat and how much is "wasted" with convective cooling) will affect ultimate lesion size.

Electrode Temperature

The electrode is passively heated by conduction of heat from the tissue during ablation. Lesion size increases directly with electrode temperature up until the point of coagulum formation and impedance rise. The relationship between lesion size and electrode temperature is confounded by the effects of convective cooling and catheter motion in vitro.

Peak Tissue Temperature

Because of convective cooling, electrode temperature underestimates peak tissue temperature—the real determinant of lesion size. Future sensors such as infrared, microwave, or ultrasound elasticity monitors may allow the operator to monitor actual lesion growth.

Electrode Contact Pressure

Greater electrode-tissue contact pressure increases lesion size by improving electrical coupling with the tissue, increasing the electrode surface area in contact with the tissue, and reducing the shunting of current to the blood pool. In addition, greater contact pressure may prevent the electrode from sliding with cardiac motion. The optimal electrode contact pressure is believed to be 20 to 40 g.[6,71] Excessive contact that buries the electrode in the tissue, however, may prevent convective cooling of the electrode and reduce current delivery.

Convective Cooling

Ultimately, lesion size is a function of tissue heating, and tissue heating is a function of the magnitude of RF power that is converted into heat in the tissues. The greater magnitude of power delivered to the tissue, the greater the lesion size. Convective cooling at the electrode-tissue interface, either active or passive, will allow the operator to safely increase the power amplitude before impedance rises. However, if the ablation is power limited (i.e., the maximal available power is delivered throughout the ablation), greater degrees of convective cooling will draw heat from the tissue to create a smaller lesion size. The two factors that affect passive cooling at the electrode-tissue interface are the magnitude of regional blood flow and the stability of the electrode catheter on the tissue surface. Catheter motion over the tissue greatly increases the loss of heat to the blood pool. Intramyocardial blood flow draws heat from the tissue and not from the electrode and therefore decreases lesion size.

Electrode Size

When the goal is to maximize lesion size, larger electrodes will always be better than smaller electrodes. Larger electrodes increase the surface area and allow the operator to deliver higher total power without excessive current density at the electrode-tissue interface. Thus, coagulum formation with a sudden rise in electrical impedance can be avoided despite high total power delivery. The higher power delivery to the tissue increases the depth of direct volume heating and in turn increases the size of the virtual heat source. This translates directly into a larger lesion. As is the case with cooled electrodes, a large electrode will result in larger lesion formation only if it is accompanied by higher power

ENDYMED EXHIBIT 1022 - 16/20

TABLE 1-2

FACTORS INFLUENCING RADIOFREQUENCY LESION SIZE

Factor	Effect on Lesion Size
Targeting	Close proximity to the target improves likelihood of success even with a small lesion size
Tissue composition	Smaller lesion sizes in scar and fat
Power	Directly proportional to lesion size
Ablation electrode temperature	Grossly proportional to lesion size but underestimates peak tissue temperature because of convective cooling effects
Peak tissue temperature	Directly proportional to lesion size
Electrode-tissue contact pressure	Directly proportional to lesion size
Convective cooling over electrode-tissue interface	
Active: perfused-tip catheter	With fixed energy delivery, reduces lesion size; with unlimited energy, increases lesion size
Passive: large tip, sliding contact	Reduces lesion size
Intramyocardial arterial flow	
Electrode size (radius and length)	Directly proportional to lesion size provided unrestricted power
Duration of energy delivery	Monoexponential relation to lesion size with half-time lesion formation of 5–10 seconds
Ablation circuit impedance	Lower body and dispersive (skin) patch resistance increases current delivery. Shunting current through blood decreases impedance but can reduced lesion size.
Electrode orientation	For nonirrigated electrode, parallel orientation increases lesion size. For irrigated electrode, perpendicular orientation increases lesion size.
Electrode geometry	Affects lesion size and shape by concentrating current density at electrode edges and asymmetries
Electrode material	Higher heat conductive materials increase lesion size by electrode cooling
Radiofrequency characteristics	
Pulsed	May increase lesion size by allowing electrode cooling
Phased	Increases continuity of linear lesions formed with multielectrode arrays
Frequency	Reduced heating efficiency at higher (MHz) frequencies

delivery. If a large electrode is employed with lower power, there may be a larger endocardial surface area ablated, but the lesion will not be as deep. RF energy delivery to multiple electrodes simultaneously may produce a large lesion as well, but other issues such as catheter and target geometry may limit energy coupling to the tissue if electrode-tissue contact is poor.

Duration of Energy Delivery

Tissue temperature follows a monoexponential rise during RF delivery (Table 1-2) until steady state is achieved. The half-time for lesion formation is 5 to 10 seconds. Therefore, lesion formation is assumed to be nearly complete after 45 to 60 seconds (five half-lives).

Ablation Circuit Impedance

By Ohm's law, lower resistance will allow for greater current delivery for the same applied voltage. For RF ablation, reducing resistance within the cables and dispersive electrode current path will increase current delivery to the tissue. The electrode-tissue interface represents two resistances in parallel, the tissue resistance and the blood pool resistance (Fig. 1-7). The resistance of the blood pool is about half that of the myocardial tissue.[72] Therefore, current preferentially flows through the blood pool from electrode surfaces not in contact with tissue. This becomes most apparent with the use of a large-tip electrode placed perpendicular to the tissue. Although the system impedance is reduced, this results in current shunting through the blood and reduced current to the tissue unless high power outputs are applied.

Electrode Orientation

For nonirrigated electrodes with unrestricted power, an orientation parallel to the tissue generally results in larger lesions because of a larger electrode area in contact with the tissue and less current shunting to the blood pool. For irrigated electrodes delivering high power outputs, the parallel electrode orientation results in smaller lesion sizes because of a greater magnitude of tissue cooling.[29]

Electrode Geometry

Very long electrodes will provide greater surface area, allow higher power delivery, and usually yield larger lesions. If the electrode is too long, however, efficiency of electrode coupling to the tissue is lost, and lesion size is not increased.[22] Also, power is concentrated at points of geometric transitions (the edge effect), resulting in the possibility of excess heating at the electrode edges and less heating in the middle of the electrode.[39]

Electrode Material

Electrode materials with high heat transfer characteristics (such as gold) are more effectively cooled by passive blood flow and may allow for greater current deliveries.[73]

ENDYMED EXHIBIT 1022 - 17/20

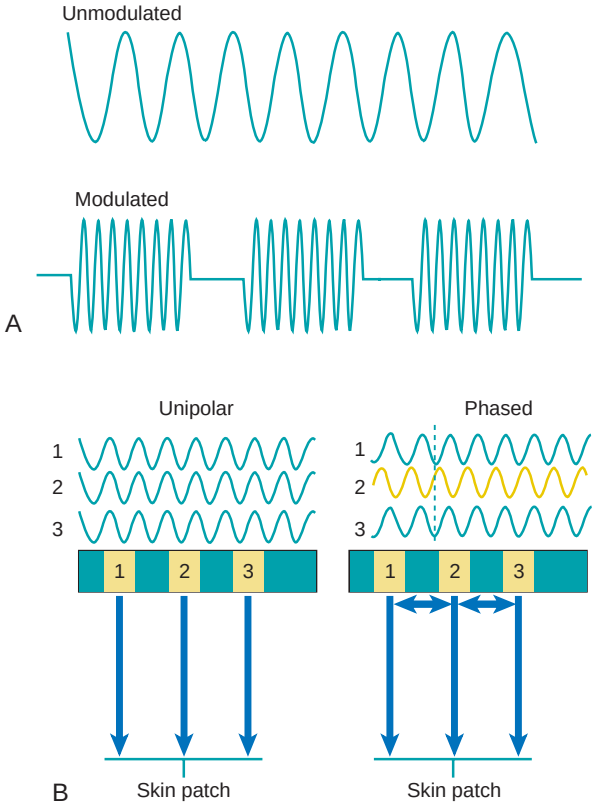

FIGURE 1-15. A, Unmodulated and modulated patterns of radiofrequency (RF) power. The modulated waveform is pulsed with periods of oscillating voltage separated by periods of quiescence. **B,** Unipolar and phased RF deliveries from a multielectrode array. With the unipolar delivery, the oscillating voltages among the electrodes are all in phase, and therefore there is no electrical potential for current flow between electrodes. With phased RF, the oscillations in voltage among contiguous electrodes are out of phase, creating an electrical potential for current to flow between electrodes as well as to the dispersive skin electrode.

Characteristics of Radiofrequency Energy

As noted, very high frequencies of alternating current lead to less efficient tissue heating, and lower frequencies may result in tissue stimulation. Pulsed RF current may allow for more electrode cooling than unmodulated RF and therefore increase power delivery (Fig. 1-15). With multielectrode ablation arrays, phased RF among the electrodes allows for more continuous linear lesions (Fig. 1-15).

Conclusion

RF catheter ablation remains the dominant modality for ablative therapy of arrhythmias. This technology is simple, has a high success rate, and has a low complication rate. Despite the fact that new ablation technologies such as ultrasound, laser, microwave, and cyrothermy are being tested and promoted as being easier, safer, or more efficacious, they are unlikely to supplant RF energy as the first choice for ablation of most arrhythmias. An appreciation of the biophysics and pathophysiology of RF energy heating of myocardium during catheter ablation will help the operator to make the proper adjustments to optimize ablation safety and success. A tissue temperature of 50°C needs to be reached to achieve irreversible tissue injury. This likely occurs as a result of sarcolemmal membrane injury and intracellular calcium overload. The 50°C isotherm determines the boundary of the lesion. Greater lesion size is achieved with higher power delivery and higher intramural tissue temperatures. Monitoring surface temperature is useful to help prevent boiling of blood with coagulum formation and a sudden increase in electrical impedance. The selection of standard versus cooled tip; 4-mm versus 5-mm, 8-mm, or 10-mm electrode-tip size; maximal power delivered; and maximal electrode-tip temperature targeted will be achieved with a full understanding of the biophysics of catheter ablation. Finally, a complete understanding of the anatomy and physiology of the arrhythmogenic substrate will allow the operator to select the optimal ablation approach.

References

1. Huang SK, Jordan N, Graham A, et al. Closed-chest catheter desiccation of atrioventricular junction using radiofrequency energy: a new method of catheter ablation [abstract]. *Circulation*. 1985;72:III–1389 (abstract).
2. Huang SK, Bharati S, Graham AR, et al. Closed-chest catheter desiccation of the atrioventricular junction using radiofrequency energy: a new method of catheter ablation. *J Am Coll Cardiol*. 1987;9:349–358.
3. Whayne JG, Nath S, Haines DE. Microwave catheter ablation of myocardium in vitro: assessment of the characteristics of tissue heating and injury. *Circulation*. 1994;89:2390–2395.
4. Haines DE, Watson DD. Tissue heating during radiofrequency catheter ablation: a thermodynamic model and observations in isolated perfused and superfused canine right ventricular free wall. *Pacing Clin Electrophysiol*. 1989;12:962–976.
5. Erez A, Shitzer A. Controlled destruction and temperature distributions in biological tissues subjected to monoactive electrocoagulation. *J Biomech Eng*. 1980;102:42–49.
6. Haines DE. Determinants of lesion size during radiofrequency catheter ablation: the role of electrode-tissue contact pressure and duration of energy delivery. *J Cardiovasc Electrophysiol*. 1991;2:509–515.
7. Wittkampf FH, Nakagawa H, Yamanashi WS, et al. Thermal latency in radiofrequency ablation. *Circulation*. 1996;93:1083–1086.
8. Haines DE, Watson DD, Verow AF. Electrode radius predicts lesion radius during radiofrequency energy heating: validation of a proposed thermodynamic model. *Circ Res*. 1990;67:124–129.
9. Schreieck J, Zrenner B, Kumpmann J, et al. Prospective randomized comparison of closed cooled-tip versus 8-mm-tip catheters for radiofrequency ablation of typical atrial flutter. *J Cardiovasc Electrophysiol*. 2002;13:980–985.
10. Tsai CF, Tai CT, Yu WC, et al. Is 8-mm more effective than 4-mm tip electrode catheter for ablation of typical atrial flutter? *Circulation*. 1999;100:768–771.
11. Kasai A, Anselme F, Teo WS, et al. Comparison of effectiveness of an 8-mm versus a 4-mm tip electrode catheter for radiofrequency ablation of typical atrial flutter. *Am J Cardiol*. 2000;86:1029–1032 A10.
12. Simmers TA, de Bakker JM, Coronel R, et al. Effects of intracavitary blood flow and electrode-target distance on radiofrequency power required for transient conduction block in a Langendorff-perfused canine model. *J Am Coll Cardiol*. 1998;31:231–235.
13. Kilicaslan F, Verma A, Saad E, et al. Transcranial Doppler detection of microembolic signals during pulmonary vein antrum isolation: implications for titration of radiofrequency energy. *J Cardiovasc Electrophysiol*. 2006;17:495–501.
14. Haines DE, Verow AF. Observations on electrode-tissue interface temperature and effect on electrical impedance during radiofrequency ablation of ventricular myocardium. *Circulation*. 1990;82:1034–1038.
15. Demolin JM, Eick OJ, Munch K, et al. Soft thrombus formation in radiofrequency catheter ablation. *Pacing Clin Electrophysiol*. 2002;25:1219–1222.
16. Wang TL, Lin JL, Hwang JJ, et al. The evolution of platelet aggregability in patients undergoing catheter ablation for supraventricular tachycardia with radiofrequency energy: the role of antiplatelet therapy. *Pacing Clin Electrophysiol*. 1995;18:1980–1990.
17. Jain MK, Wolf PD. A three-dimensional finite element model of radiofrequency ablation with blood flow and its experimental validation. *Ann Biomed Eng*. 2000;28:1075–1084.
18. Strickberger SA, Hummel J, Gallagher M, et al. Effect of accessory pathway location on the efficiency of heating during radiofrequency catheter ablation. *Am Heart J*. 1995;129:54–58.
19. Kalman JM, Fitzpatrick AP, Olgin JE, et al. Biophysical characteristics of radiofrequency lesion formation in vivo: dynamics of catheter tip-tissue contact evaluated by intracardiac echocardiography. *Am Heart J*. 1997;133:8–18.

ENDYMED EXHIBIT 1022 - 18/20

20. Nakagawa H, Yamanashi WS, Pitha JV, et al. Comparison of in vivo tissue temperature profile and lesion geometry for radiofrequency ablation with a saline-irrigated electrode versus temperature control in a canine thigh muscle preparation. *Circulation*. 1995;91:2264–2273.
21. Mukherjee R, Laohakunakorn P, Welzig MC, et al. Counter intuitive relations between in vivo RF lesion size, power, and tip temperature. *J Interv Cardiac Electrophysiol*. 2003;9:309–315.
22. Petersen HH, Chen X, Pietersen A, et al. Lesion dimensions during temperature-controlled radiofrequency catheter ablation of left ventricular porcine myocardium: impact of ablation site, electrode size, and convective cooling. *Circulation*. 1999;99:319–325.
23. Otomo K, Yamanashi WS, Tondo C, et al. Why a large tip electrode makes a deeper radiofrequency lesion: effects of increase in electrode cooling and electrode-tissue interface area. *J Cardiovasc Electrophysiol*. 1998;9:47–54.
24. Dorwarth U, Fiek M, Remp T, et al. Radiofrequency catheter ablation: different cooled and noncooled electrode systems induce specific lesion geometries and adverse effects profiles. *Pacing Clin Electrophysiol*. 2003;26:1438–1445.
25. Spitzer SG, Karolyi L, Rammler C, Otto T. Primary closed cooled tip ablation of typical atrial flutter in comparison to conventional radiofrequency ablation. *Europace*. 2002;4:265–271.
26. Atiga WL, Worley SJ, Hummel J, et al. Prospective randomized comparison of cooled radiofrequency versus standard radiofrequency energy for ablation of typical atrial flutter. *Pacing Clin Electrophysiol*. 2002;25:1172–1178.
27. Everett TH 4th, Lee KW, Wilson EE, et al. Safety profiles and lesion size of different radiofrequency ablation technologies: a comparison of large tip, open and closed irrigation catheters. *J Cardiovasc Electrophysiol*. 2009;20:325–335.
28. Watanabe I, Masaki R, Min N, et al. Cooled-tip ablation results in increased radiofrequency power delivery and lesion size in the canine heart: importance of catheter-tip temperature monitoring for prevention of popping and impedance rise. *J Interv Cardiac Electrophysiol*. 2002;6:9–16.
29. Wood MA, Goldberg SM, Parvez B, et al. Effect of electrode orientation on lesion sizes produced by irrigated radiofrequency ablation catheters. *J Cardiovasc Electrophysiol*. 2009;20:1262–1268.
30. Fuller IA, Wood MA. Intramural coronary vasculature prevents transmural radiofrequency lesion formation: implications for linear ablation. *Circulation*. 2003;107:1797–1803.
31. Ko WC, Huang SK, Lin JL, et al. New method for predicting efficiency of heating by measuring bioimpedance during radiofrequency catheter ablation in humans. *J Cardiovasc Electrophysiol*. 2001;12:819–823.
32. Thiagalingam A, D'Avila A, McPherson C, et al. Impedance and temperature monitoring improve the safety of closed-loop irrigated-tip radiofrequency ablation. *J Cardiovasc Electrophysiol*. 2007;18:318–325.
33. Seiler J, Roberts-Thomson KC, Raymond JM, et al. Steam pops during irrigated radiofrequency ablation: feasibility of impedance monitoring for prevention. *Heart Rhythm*. 2008;5:1411–1416.
34. Jain MK, Wolf PD. Temperature-controlled and constant-power radiofrequency ablation: what affects lesion growth? *Trans Biomed Eng*. 1999;46:1405–1412.
35. McRury ID, Whayne JG, Haines DE. Temperature measurement as a determinant of tissue heating during radiofrequency catheter ablation: an examination of electrode thermistor positioning for measurement accuracy. *J Cardiovasc Electrophysiol*. 1995;6:268–278.
36. Liu Z, Ahmed M, Weinstein Y, et al. Characterization of the RF ablation-induced "oven effect": the importance of background tissue thermal conductivity on tissue heating. *Int J Hypertherm*. 2006;22:327–342.
37. Jain MK, Tomassoni G, Riley RE, Wolf PD. Effect of skin electrode location on radiofrequency ablation lesions: an in vivo and a three-dimensional finite element study. *J Cardiovasc Electrophysiol*. 1998;9:1325–1335.
38. Nath S, DiMarco JP, Gallop RG, et al. Effects of dispersive electrode position and surface area on electrical parameters and temperature during radiofrequency catheter ablation. *Am J Cardiol*. 1996;77:765–767.
39. McRury ID, Panescu D, Mitchell MA, Haines DE. Nonuniform heating during radiofrequency catheter ablation with long electrodes: monitoring the edge effect. *Circulation*. 1997;96:4057–4064.
40. Huang SK, Bharati S, Graham AR, et al. Closed chest catheter desiccation of the atrioventricular junction using radiofrequency energy: a new method of catheter ablation. *J Am Coll Cardiol*. 1987;9:349–358.
41. Butcher RG. The measurement in tissue sections of the two formazans derived from nitroblue tetrazolium in dehydrogenase reactions. *Histochem J*. 1978;10:739–744.
42. Langberg JJ, Calkins H, el Atassi R, et al. Temperature monitoring during radiofrequency catheter ablation of accessory pathways [see comment]. *Circulation*. 1992;86:1469–1474.
43. Nath S, DiMarco JP, Mounsey JP, et al. Correlation of temperature and pathophysiological effect during radiofrequency catheter ablation of the AV junction. *Circulation*. 1995;92:1188–1192.
44. Langberg JJ, Calkins H, Kim YN, et al. Recurrence of conduction in accessory atrioventricular connections after initially successful radiofrequency catheter ablation. *J Am Coll Cardiol*. 1999;7:1588–1592.
45. DeLacey WA, Nath S, Haines DE, et al. Adenosine and verapamil-sensitive ventricular tachycardia originating from the left ventricle: radiofrequency catheter ablation [see comment]. *Pacing Clin Electrophysiol*. 1992;15:2240–2244.
46. Huang SK, Bharati S, Lev M, Marcus FI. Electrophysiologic and histologic observations of chronic atrioventricular block induced by closed-chest catheter desiccation with radiofrequency energy. *Pacing Clin Electrophysiol*. 1987;10:805–816.
47. Avitall B, Urbonas A, Urboniene D, et al. Time course of left atrial mechanical recovery after linear lesions: normal sinus rhythm versus a chronic atrial fibrillation dog model [see comment]. *J Cardiovasc Electrophysiol*. 2000;11:1397–1406.
48. Nath S, Redick JA, Whayne JG, Haines DE. Ultrastructural observations in the myocardium beyond the region of acute coagulation necrosis following radiofrequency catheter ablation. *J Cardiovasc Electrophysiol*. 1994;5:838–845.
49. Nath S, Whayne JG, Kaul S, et al. Effects of radiofrequency catheter ablation on regional myocardial blood flow: possible mechanism for late electrophysiological outcome. *Circulation*. 1994;89:2667–2672.
50. Duong T, Hui P, Mailhot J. Acute right coronary artery occlusion in an adult patient after radiofrequency catheter ablation of a posteroseptal accessory pathway. *J Invasive Cardiol*. 2004;16:657–659.
51. Sassone B, Leone O, Martinelli GN, Di Pasquale G. Acute myocardial infarction after radiofrequency catheter ablation of typical atrial flutter: histopathological findings and etiopathogenetic hypothesis. *Ital Heart J*. 2004;5:403–407.
52. Schmidt M, Nölker G, Marschang H, et al. Incidence of oesophageal wall injury post-pulmonary vein antrum isolation for treatment of patients with atrial fibrillation. *Europace*. 2008;10:205–209.
53. Helms A, West JJ, Patel A, et al. Real-time rotational ICE imaging of the relationship of the ablation catheter tip and the esophagus during atrial fibrillation ablation. *J Cardiovasc Electrophysiol*. 2009;20:130–137.
54. Evonich RF, Nori DM, Haines DE. A randomized trial comparing effects of radiofrequency and cryoablation on the structural integrity of esophageal tissue. *J Interv Card Electrophysiol*. 2007;19:77–83.
55. Sacher F, Monahan KH, Thomas SP, et al. Phrenic nerve injury after atrial fibrillation catheter ablation: characterization and outcome in a multicenter study. *J Am Coll Cardiol*. 2006;47:2498–2503.
56. Pisani CF, Hachul D, Sosa E, Scanavacca M. Gastric hypomotility following epicardial vagal denervation ablation to treat atrial fibrillation. *J Cardiovasc Electrophysiol*. 2008;19:211–213.
57. Saad EB, Marrouche NF, Saad CP, et al. Pulmonary vein stenosis after catheter ablation of atrial fibrillation: emergence of a new clinical syndrome [see comment] [summary for patients in *Ann Intern Med*. 2003;138:1; PMID: 12693916]. *Ann Intern Med*. 2003;138:634–638.
58. Kok LC, Everett TH, Akar JG, Haines DE. Effect of heating on pulmonary veins: how to avoid pulmonary vein stenosis. *J Cardiovasc Electrophysiol*. 2003;14:250–254.
59. Bromer RH, Mitchell JB, Soares N. Response of human hematopoietic precursor cells (CFUc) to hyperthermia and radiation. *Cancer Res*. 1982;42:1261–1265.
60. Lepock JR. Involvement of membranes in cellular responses to hyperthermia. *Radiat Res*. 1982;92:433–438.
61. Stevenson AP, Galey WR, Tobey RA, et al. Hyperthermia-induced increase in potassium transport in Chinese hamster cells. *J Cell Physiol*. 1983;115:75–86.
62. Nath S, Lynch III C, Whayne JG, Haines DE. Cellular electrophysiological effects of hyperthermia on isolated guinea pig papillary muscle: implications for catheter ablation. *Circulation*. 1993;88:1826–1831.
63. Coakley WT. Hyperthermia effects on the cytoskeleton and on cell morphology. *Symp Soc Exp Biol*. 1987;41:187–211.
64. Warters RL, Henle KJ. DNA degradation in Chinese hamster ovary cells after exposure to hyperthermia. *Cancer Res*. 1982;42:4427–4432.
65. Warters RL, Roti Roti JL. Hyperthermia and the cell nucleus. *Radiat Res*. 1982;92:458–462.
66. Warters RL, Brizgys LM, Sharma R, Roti Roti JL. Heat shock (45 degrees C) results in an increase of nuclear matrix protein mass in HeLa cells. *Int J Radiat Biol*. 1986;50:253–268.
67. Everett TH, Nath S, Lynch III C, et al. Role of calcium in acute hyperthermic myocardial injury. *J Cardiovasc Electrophysiol*. 2001;12:563–569.
68. Simmers TA, de Bakker JM, Wittkampf FH, Hauer RN. Effects of heating on impulse propagation in superfused canine myocardium. *J Am Coll Cardiol*. 1995;25:1457–1464.
69. Simmers TA, de Bakker JM, Wittkampf FH, Hauer RN. Effects of heating with radiofrequency power on myocardial impulse conduction: is radiofrequency ablation exclusively thermally mediated? *J Cardiovasc Electrophysiol*. 1996;7:243–247.
70. Hong KN, Russo MJ, Liberman EA, et al. Effect of epicardial fat on ablation performance: a three-energy source comparison. *J Card Surg*. 2007;22:521–524.
71. Yokoyama K, Nakagawa H, Shah D, et al. Novel contact force sensor incorporated in irrigated radiofrequency ablation catheter predicts lesion size and incidence of steam pop and thrombus. *Circ Arrhythm Electrophysiol*. 2008;1:354–362.
72. Wittkampf FHM, Nakagawa H. RF catheter ablation: lessons on lesions. *Pacing Clin Electrophysiol*. 2006;29:1285–1297.
73. Linhart M, Mollnau H, Bitzen A, et al. In vitro comparison of platinum-iridium and gold tip electrodes: lesion depth in 4 mm, 8 mm, and irrigated-tip radiofrequency ablation catheters. *Europace*. 2009;11:565–570.

ENDYMED EXHIBIT 1022 - 19/20

Videos

Video 1-1. Infrared thermal imaging of tissue heating during radiofrequency ablation with a closed irrigation catheter as seen from the surface of the tissue. Power is delivered at 30 W to blocks of porcine myocardium in a tissue bath. The surface of the tissue is just above the fluid level to permit thermal imaging of tissue and not the fluid. Temperature scale (*right*) and a millimeter scale (*top*) are shown in each panel.

Video 1-2. Infrared thermal imaging of tissue heating during radiofrequency ablation with a closed irrigation catheter as seen in cross section. Power is delivered at 30 W to blocks of porcine myocardium in a tissue bath. The surface of the tissue is just above the fluid level to permit thermal imaging of tissue and not the fluid. Temperature scale (*right*) and a millimeter scale (*top*) are shown in each panel.

ENDYMED EXHIBIT 1022 - 20/20